Capillary Wave Studies of Polystyrene-*b*-poly(methacrylic acid) Diblock Copolymer Films at the Toluene/Water Interface

S. E. May-Colaianni, J. V. Gandhi, K. J. Måløy, and J. V. Maher*

Department of Physics and Astronomy, University of Pittsburgh, Pittsburgh, Pennsylvania 15260

K. A. Kuhar and T. M. Chapman

Department of Chemistry, University of Pittsburgh, Pittsburgh, Pennsylvania 15260

*Received December 23, 1992; Revised Manuscript Received August 17, 1993**

ABSTRACT: We have used both a mechanically generated capillary wave technique and surface light scattering to measure capillary wave properties of the toluene/water interface covered by polystyrene-*b*-poly(methacrylic acid) diblock copolymer (PS–PMAA) as a function of both the overall molecular weight M_w and the interfacial concentration of the diblock copolymer. As interfacial polymer number density N is increased, surface pressure π increases with a slope dependent on molecular weight and reaches a maximum value at a particular interfacial density (saturation density), beyond which density π no longer changes appreciably. The slope of $\pi(N)$ indicates that all molecular weights show approximately the same areal compressibility at the lowest number densities. The saturation surface pressure increases with molecular weight.

I. Introduction

There is growing experimental literature on the behavior of copolymers at air–liquid interfaces.[1-9] Recent reports show that, in such cases, interesting two-dimensional micelle-like structures may be formed and intriguing viscoelastic surface properties can be observed.[7-10] However, there is very little experimental work available for copolymer films on liquid–liquid interfaces.[11,12] While such cases are much harder to measure, they afford an opportunity to work with films in which neither polymer block is collapsed and in fact where the quality of both solvents can, at least in principle, be modified. In this paper, we report measurements of diblocks at an interface between immiscible liquids, each of which is a good solvent for one of the blocks.

We have measured the capillary wave dispersion relation for the toluene/water interface covered with polystyrene-*b*-poly(methacrylic acid) diblock copolymer (PS–PMAA). Both mechanically generated capillary waves[13] and surface light scattering from thermally driven waves have been measured to provide the dispersion relation for the waves on these interfaces over a wide frequency/wavenumber range. We have used these measurements to obtain values for the interfacial viscoelastic parameters as a function of polymer molecular weight and interfacial number density. Section II contains a description of the polymer and solvent preparation along with a discussion of the details of the two capillary wave measurements. Section III begins with a description of the conditions under which reproducible data could be measured and follows with detailed discussions of the analyses of driven capillary wave data and surface light scattering data. In section IV, measured surface pressures and surface viscosities are presented as functions of polymer molecular weight and number density. Section IV also contains a discussion of the low-polymer-number-density compressibility and the high-polymer-number-density surface pressure, with implications for polymer conformation if all, or most, of the polymer molecules were to join as interfacial monolayer.

II. Experimental Section

A. Materials. Methanol (Mallinckrodt) and dimethyl sulfoxide (Fisher) were distilled before use. 1,4-Dioxide (Fisher) was distilled from sodium. The water used was doubly distilled (DD water) from a basic permanganate solution.

Table I. Molecular Weight Data for PS–PMMA Copolymers

sample	M_p[a]	M_w/M_n[a]	M_w[b]	M_w/M_n[b]
14K.603	14 000	1.09	14 500	1.10
38K.395	37 600	1.10	38 600	1.13
283K.415	283 400	1.09	273 000	1.09

[a] From Polymer Laboratories. [b] Determined by GPC versus calibration with polystyrene standards.

The polystyrene-*b*-poly(methacrylic acid) (PS–PMAA) diblock copolymers used in this experiment were prepared by hydrolysis of polystyrene-*b*-poly(methyl methacrylate) (PS–PMMA) diblock copolymers purchased from Polymer Laboratories.[14] Gel permeation chromatography (GPC) was used to determine the molecular weights and molecular weight distributions of the PS–PMMA copolymers. The values reported are relative to a polystyrene standard calibration. Table I summarizes the molecular weight data for these copolymers.

The PS–PMMA copolymers were hydrolyzed by KOH in 1,4-dioxane/methanol.[15] Typically, the copolymer was dissolved in 1,4-dioxane and a 5–10% excess of KOH, relative to MMA content, was added as a 20% solution in methanol. The solution was purged with nitrogen and then refluxed for 48–76 h. During this time the initially homogeneous solution became heterogeneous. The PS–PMAA was recovered by pouring the suspension into an excess of DD water and acidifying with concentrated HCl. The precipitate formed was recovered by either filtering or centrifuging the suspension and washing several times with additional DD water. The final polymers were dried under vacuum at 65 °C for 24 h.

The degree of hydrolysis and the relative monomer composition of the PS–PMAA copolymers were determined by ^{1}H NMR in DMSO-d_6 at 363 K using a Bruker 300-MHz spectrometer. These results are summarized in Table II.

B. Methods. We used a technique developed by Måløy et al.[13] to mechanically generate capillary waves (MGCW), and we measured capillary wave profiles using the laser deflection technique of Leiderer et al.[16] An ac current was passed through a 50-μm-diameter Pt wire, placed parallel to and less than ~0.5 mm below the toluene/water interface. A horseshoe-shaped magnet was placed over the wire, just above the toluene phase, which caused the wire to oscillate vertically when ac current was passed through the wire. As shown in Figure 1, light from a

* Abstract published in *Advance ACS Abstracts*, October 15, 1993.

0024-9297/93/2226-6595$04.00/0

Table II. Results from Hydrolysis of PS–PMMA Copolymers with KOH in 1,4-Dioxane/Methanol

sample	label[a]	PS/PMMA[b]	PS/PMAA[b]	yield of hydrolysis,[c] %
14K.603	50:50	42:58	42:52	95.4
38K.395	47.0:53.0	47:53[d]	47:48	96.6
283K.415	42.5:57.5	42:58	43:57	89.8

[a] PS/PMMA from Polymer Laboratories. [b] From ^{1}H NMR in DMSO-d_6 at 363 K. Determined from integration of the aromatic protons of PS and the α-methyl protons of PMMA or PMAA. [c] Determined from integration of the methyl protons of any remaining ester (unreacted MMA) and the α-methyl protons of PMAA. [d] From ^{1}H NMR in $CDCl_3$.

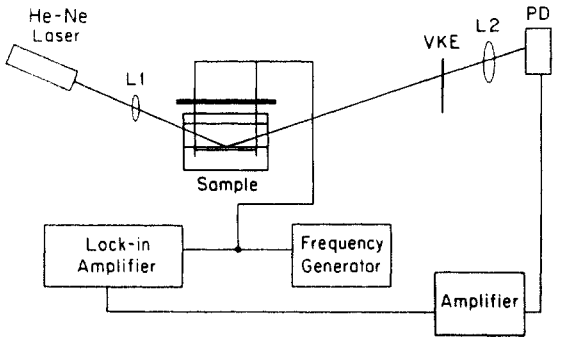

Figure 1. Experimental schematic for mechanically generated capillary wave (MGCW) measurements.

632.8-nm He–Ne laser was focused onto the interface by lens L1 and was reflected from the interface between the toluene and water phases, which were held in a Pyrex glass container.[17] A vertical knife edge (VKE) was positioned so that when the wire was at rest, half of the exciting reflected beam passed by it, and this light was focused by lens L2 onto a photodiode (PD). The photodiode signal was amplified and sent to a lock-in amplifier, with the ac signal driving the oscillating wire serving as the reference signal for the lock-in amplifier. As is discussed in refs 13 and 18, for a damped traveling wave, $\xi(x, t)$, of complex wavenumber $q^* = q - i\beta$, the total deflection of the laser beam is proportional to the instantaneous slope of the wave profile $\partial\xi/\partial x$ and the output of the photodiode is

$$V_1(x, t) = 2\chi I_0 R \sin\theta \left.\frac{\partial \xi}{\partial x}\right|_{x,t} \propto \left.\frac{\partial \xi}{\partial x}\right|_{x,t} \quad (1)$$

where χ is the photodiode response, I_0 the total power from the laser, R the distance from the point of interfacial reflection to the knife edge, and θ the angle between the interface and the laser beam. From the instantaneous slope information contained in $V_1(x,t)$, the lock-in amplifier extracts the part of the signal which correlates with the driving/reference signal to yield a spatial wave form

$$V(x) = A(q^2 + \beta^2)^{1/2} e^{-\beta x} \cos(qx + \phi) \quad (2)$$

where A is a constant proportional to the amplitude of the interfacial wave. Using this technique to measure $V(x)$, we have typically extracted values of q and β for frequencies in the range 500–2900 Hz.

We also used dynamic surface light scattering (SLS)[19] to determine the complex frequency $f^* = \omega^*/2\pi = f_0 + i(\Delta f/2)$ of thermally generated capillary waves at typically five different wavenumbers in the range 350–1400 cm^{-1}. Figure 2 shows a diagram of the apparatus used in these measurements. An argon ion laser beam was passed through a spatial filter (L1 + P1 + L2) and a Ronchi ruling which separated the beam into diffraction orders. Lens L4 was positioned so that the diffraction orders converged at the interface. Pinhole P2 was used to select light scattered in a particular direction, corresponding to a coherent mixture of scattered light at one wavenumber with the specularly reflected light from one diffraction order. The selected scattered light was focused (using lens L3) onto the detector and passed through pinhole P3 (which aided in eliminating light from other sources). The detector was an RCA SPCM 100 photon counting photodiode, and the (heterodyne) autocorrelation function of

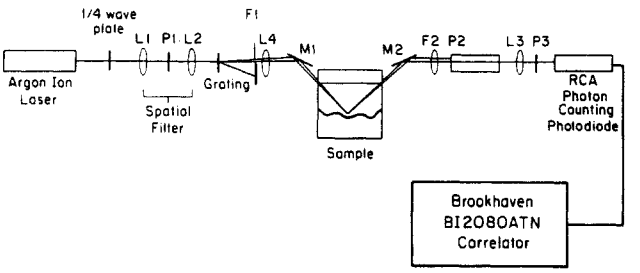

Figure 2. Experimental schematic for surface light scattering (SLS) experiments.

detected photons was constructed by a Brookhaven BI-2030AT correlator. This autocorrelation function was later Fourier transformed to yield the power spectrum for capillary relaxation whose mean peak value and peak half-width yield $f_o(q)$ and $\Delta f(q)$ for the capillary waves. Typically, measurements were made at five distinct values of the wavenumber q, each corresponding to using one of the available diffraction orders as a reference beam for heterodyning. All experiments were performed on a vibration isolation table (Newport KNS Series) to isolate the system from external low frequency disturbances (~0.2–5 Hz).

III. Data Analysis

In the data below, the total number of polymer molecules which have been incorporated in a given sample is presented as an areal number density as if all molecules are located on the toluene–water interface. It is difficult to measure the solubility of PS–PMAA in either toluene or water at concentrations as low as have been used in the experiment, and thus our light scattering measurements have yielded only qualitative results which indicate, quite plausibly, that for global concentrations of interest here many fewer molecules go into solution in water below a toluene–water interface than dissolve in water below an air–water interface. In the discussion section below (section IV), arguments will be presented which imply that at the higher polymer concentrations it is highly likely that some of the polymer either goes into solution (as individual molecules or as micelles) or possibly forms multilayered structures on the interface rather than further crowd the single-layered interface. Despite these possible problems, it is convenient to present the data with polymer concentration listed as an interfacial number density. The measured capillary wave spectra were very reproducible within the uncertainties discussed below, suggesting that a consistent fraction of the polymer stayed on the interface for each sample. Tipping the sample back and forth could change the capillary wave spectra (always in the direction of spectra seen for undisturbed samples with less polymer), indicating that polymer would adhere to the glass walls of the sample container if the liquid interface was moved along the container wall. All measurements discussed below were reproducible as long as samples were prepared according to the prescription described in the next paragraph and care was taken not to agitate the interface.

Samples were prepared by adding the appropriate number of drops of stock solution of copolymer in DMSO to the water–air interface and subsequently adding toluene to the interface. When samples were prepared in this way, capillary wave spectra reached their "equilibrium" values within approximately half an hour after the toluene was added and then showed no changes with time when observed for as much as 48 h. Typically, polymer–DMSO drops were added at several different places on the water–air interface and the results were not sensitive to the exact position or the number of such positions, unless all polymer drops were added to just one position, in which case the system became trapped in a long-lived metastable state

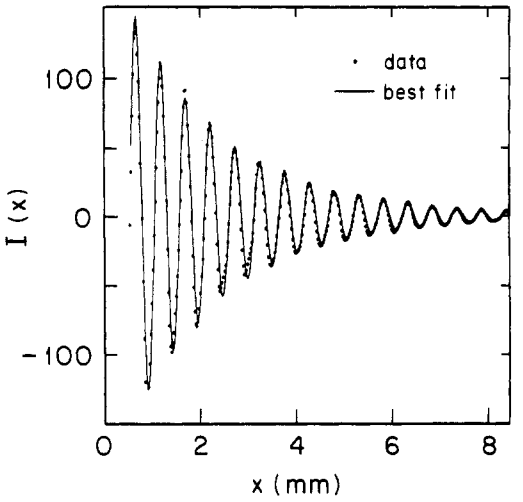

Figure 3. Measured capillary wave profile $I(x)$ versus distance x between disturbing wire and point of laser reflection, for capillary wave frequency 900 Hz, at 116 × 10^{12} molecules/cm² of 38K M_w PS–PMAA diblock copolymer.

whose surface tension could be as much as ~15% different from that of the state we are assuming to be the equilibrium state. (Metastability was also observed when polymer was added to the air–toluene interface and allowed to fall on the water–toluene interface. All data presented in this paper resulted from samples prepared by adding polymer to water–air interface before adding toluene.)

No significant difference in the interfacial properties was observed if a short or long time elapsed between adding polymer to the air–water interface and adding toluene to the combined system. At high polymer concentration, adding polymer to the air–water interface could lead, depending on the molecular weight and concentration, to either or both of scattering centers in the bulk water (presumably micelles) and visible "islands" of opaqueness on the interface (presumably a condensed polymer phase).[7-10] However, both kinds of inhomogeneity dissolved away within approximately an hour after toluene was added to the system and the resulting interface showed no observable dependence on how long the scattering centers had been allowed to evolve before the toluene was added. Properties of the air–water interface will be presented elsewhere and are mentioned here only because they suggest both that the samples reach a resonably robust equilibrium and that the copolymer may be strongly attached to the toluene–water interface.

A. Mechanically Generated Capillary Wave Technique. Each measured capillary wave profile obtained using the MGCW technique was fitted, using a least-squares method, to the form

$$I(x) = ae^{-\beta x}\cos(qx + \phi) \tag{3}$$

where x is the distance from the wire. A measured capillary wave profile and its least-squares fit are shown in Figure 3. The least-square fits for q and β for a single measured wave form gave very small uncertainties, but by repeating measurements we found that q and β are reproducible for any one sample to 0.25% and 10%, respectively. (The uncertainty in β is larger because fewer characteristic damping lengths, $1/\beta$, are observable than oscillation lengths, $2\pi/q$.) Figure 4 shows our measured values for q and β as a function of frequency for various surface densities of the 14K M_w diblock copolymer. We find that both q and β tend to increase with increasing polymer density until reaching maximum values around 400 × 10^{12} molecules/cm². We also observe for polymer of M_w = 38K

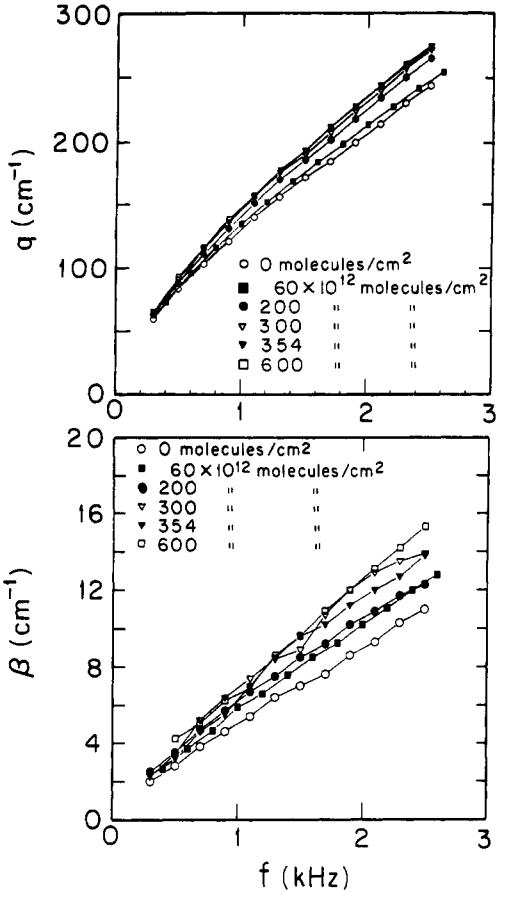

Figure 4. Measured values for the wavenumber q and spatial damping constant β as a function of frequency, at various values of the interfacial polymer concentration for the 14K M_w PS–PMAA diblock copolymer. The error bars for q are in each case smaller than the data symbol shown. Typically uncertainties for β are approximately 10%.

and 283K that q and β tend to increase with increasing number density, reaching maximum values around 160 × 10^{12} molecules/cm² and 20 × 10^{12} molecules/cm², respectively.

B. Dispersion Relation. The capillary wave dispersion relation for a thin viscoelastic interface between two simple liquids has been reported by Lucassen-Reynders and Lucassen.[20] Since there is not enough polymer in any of our samples to produce an appreciable change in the viscosity of water or toluene and since the shortest wavelength we measure is very long in comparison with the thickness of any interfacial zone which our polymer could form, this dispersion relation is appropriate for the present experiment and we need not consider the more complicated relations which might otherwise be applicable.[21,54] If we let ρ_1 and η_1 be the density and viscosity of the upper liquid (toluene) and ρ_2 and η_2 be the density and viscosity of the lower liquid (water) and we define $m_1 = (q^{*2} + i(\omega\rho_1/\eta_1))^{1/2}$ for the upper liquid and $m_2 = (q^{*2} + i(\omega\rho_2/\eta_2))^{1/2}$ for the lower liquid with $\omega = 2\pi f$, we can construct functions

$$E = \frac{\epsilon^* q^{*2}}{\omega} + i[\eta_2(q^* + m_2) + \eta_1(q^* + m_1)] \tag{4}$$

$$S = \frac{\sigma^* q^{*2}}{\omega} + i[\eta_2(q^* + m_2) + \eta_1(q^* + m_1)] + \frac{g(\rho_2 - \rho_1)}{\omega} - \frac{\omega(\rho_2 + \rho_1)}{q^*} \tag{5}$$

where $\epsilon^* = \epsilon + i\omega\kappa$ is the complex dilational elastic modulus and $\sigma^* = \sigma + i\omega\mu$ is the complex surface tension. The

capillary wave dispersion relation can then be written

$$D = [\eta_2(q^* - m_2) - \eta_1(q^* - m_1)]^2 + E \cdot S = 0 \quad (6)$$

To determine viscoelastic parameters for the interface, it is necessary to insert our measured $q(f)$ and $\beta(f)$ into $D(q^*,\omega,\sigma^*,\epsilon^*)$ and adjust σ^* and ϵ^* to satisfy $D = 0$. To accomplish this, we defined a χ^2, a weighted square fluctuation of D from its expected value of 0, as

$$\chi^2 = \sum_{i=1}^{N} \frac{|D_i(q^*_i,\omega_i,\sigma^*,\epsilon^*)|^2}{\delta_{|D_i|}^2} \quad (7)$$

where D_i is the left-hand side of eq 6 evaluated for the ith data point $q^*(\omega_i)$ and $\delta_{|D_i|}^2$ is an expected uncdertainty in D_i based on the measured uncertainties in q^*_i and ω_i. We arbitrarily chose to treat the uncertainties in q_i and β_i as independent, and since the uncertainty in ω *is* negligible compared to q_i and β_i, we write

$$\delta_{|D_i|}^2 = \left(\left.\frac{\partial D}{\partial q}\right|_{q_i,\beta_i,f_i,\sigma^*,\epsilon^*} \delta q_i\right)^2 + \left(\left.\frac{\partial D}{\partial \beta}\right|_{q_i,\beta_i,f_i,\sigma^*,\epsilon^*} \delta\beta_i\right)^2 \quad (8)$$

We minimized χ^2 using the Marquardt–Levenburg algorithm.[22] The ambient temperature throughout the experiment was 24 ± 1 °C. This introduces a small uncertainty in the viscosity of each of the bulk liquids. Thus it is necessary to increase the uncertainties in the interfacial viscoelastic parameters to a total value for each parameter i of

$$\Delta_i = ((\Delta_i)_{calc}^2 + (\Delta_i)_T^2)^{1/2} \quad (9)$$

where $(\Delta_i)_{calc}$ is the uncertainty obtained from the Marquardt–Levenburg algorithm at 24 °C and $(\Delta_i)_T$ is the change in the best-fit value of the ith parameter obtained when the liquid viscosities were changed to correspond to a 1 °C temperature fluctuation. Figure 5 compares the measured values for the wavenumber q and the damping constant β with a line calculated using eq 6 and the best-fit parameters σ, μ, κ, and ϵ at 162×10^{12} molecules/cm^2 of 38K M_w PS–PMAA diblock copolymer.

Measurement of capillary waves over a broad wavenumber and frequency range allows surface tension to be determined to ±0.2 dyn/cm in any one measurement, and as was discussed above, the surface tension measured for any one sample is very reproducible over many tens of hours. Reproducibility is slightly less good, however, if different samples of the same nominal polymer concentration are measured. Investigation of a series of samples has shown that the uncertainty in the surface tension is ±1 dyn/cm for concentrations where surface tension is not changing rapidly with concentration and slightly higher (~1.2 dyn/cm) where the surface tension changes significantly with concentration. The uncertainties shown for the data presented in section IV below include this added uncertainty from comparing different samples.

Thus we have used the parameter dependences of eq 6 and our measured dispersion relations $q(f)$, $\beta(f)$ (MGCW) and $f_o(q)$ $\Delta f(q)$ (SLS) to determine values for the interfacial viscoelastic parameters σ, μ, ϵ, and κ. Since water and toluene do not have a very large density difference and bulk viscosity difference, it was always clear from eq 6 and from discussions in the literature[19] that this experiment would have a very weak sensitivity to the longitudinal wave parameters ϵ and κ. However, it was hoped that, by combining MGCW and SLS to measure the dispersion relation over a very large range of frequency and wavenumber, it would become possible to give at least crude values of these parameters. Unfortunately, as is discussed below, only extremely crude determinations of the longitudinal parameters have been achieved even with our very large range of measured q and ω.

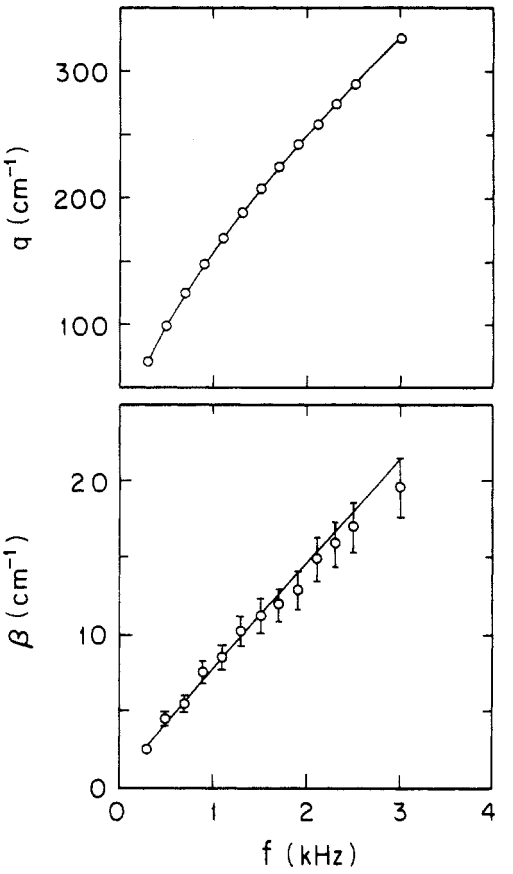

Figure 5. Measured values (open circles) and best-fit line for the wavenumber and damping constant for 162×10^{12} molecules/cm^2 of 38K M_w PS–PMMA diblock copolymer as a function of frequency. Measurement uncertainties are indicated wherever they exceed the size of the data symbol.

Only a few SLS cases were measured because analysis of these showed that the added range of frequencies did not give significantly greater sensitivity to viscoelastic parameters, i.e., the extracted values of σ^* confirmed the MGCW analysis in each case and the large uncertainties in ϵ^* were not significantly reduced. We discuss the analysis of these few SLS cases in the next subsection before presenting the main results of this paper, namely, the dependence of viscoelastic parameters on polymer molecular weight and number density.

C. Surface Light Scattering. A typical autocorrelation function and its corresponding power spectrum, at wavenumber $q = 678.5$ cm^{-1} for 35×10^{12} molecules/cm^2 of 38K M_w PS–PMAA diblock copolymer are shown in Figure 6. The power spectra $P(f)$ were fitted using a least-squares method to a Lorentzian form[19]

$$P(f) = \frac{a}{(f - f_o)^2 + (\Delta f/2)^2} \quad (10)$$

where a is a constant, f_o is the peak frequency, and Δf is the full width at half-maximum amplitude. The least-squares fits to each power spectrum gave uncertainties for the peak frequencies of approximately 1% and for the half-maximum widths of approximately 10%. An instrumental broadening correction should be made to the half-

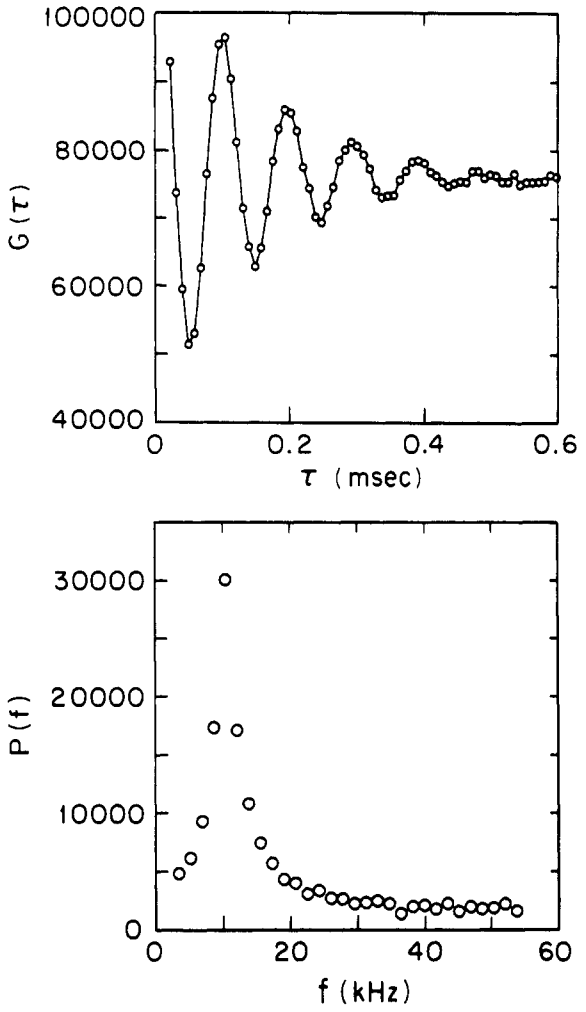

Figure 6. Measured SLS autocorrelation function $G(\tau)$ at wavenumber q = 678.5 cm^{-1} (top) and power spectrum $P(f)$ resulting from its Fourier inverse transform (bottom), at 35 × 10^{12} molecules/cm^2 of 38K M_w PS–PMAA diblock copolymer.

maximum widths of all the power spectra[11]

$$\Delta f_{inst} \approx \Delta q \left(\frac{df_o}{dq}\right) \approx [2\pi \cos(\theta_i)\Delta\theta/\lambda] \left(\frac{df_o}{dq}\right) \quad (11)$$

Here θ_i is the incident angle of the laser beam with respect to the normal to the interface, λ is the laser wavelength, $\Delta\theta$ is the angle subtended by a particular diffraction order's effective width at the defining aperture, and the derivative is the measured rate of change of peak frequency f_o with wavenumber q. The corrected half-maximum width, Δf_c, should in principle be calculated as[23]

$$\Delta f_c \approx \Delta f_{exper} - (\Delta f_{inst}^2/\Delta f_{exper}) \quad (12)$$

where Δf_{exper} is the experimentally measured half-maximum width. As has been reported for other SLS experiments,[19] the instrumental width would have to be increased significantly from its measured value to avoid having the data lead to a frequency-dependent value of the transverse viscosity μ, even for the bare (no polymer) interface. This problem makes the SLS determination of μ inherently less reliable than the determination which results from the MGCW measurement. While the SLS measurement never shows a serious discrepancy with the MGCW measurement, only the MGCW results for μ are presented below. No such problem exists for the surface tension determination.

SLS peak frequencies were found to decrease gradually with increasing polymer number density, as is shown in Figure 7 for the polymer of molecular weight 38K. These

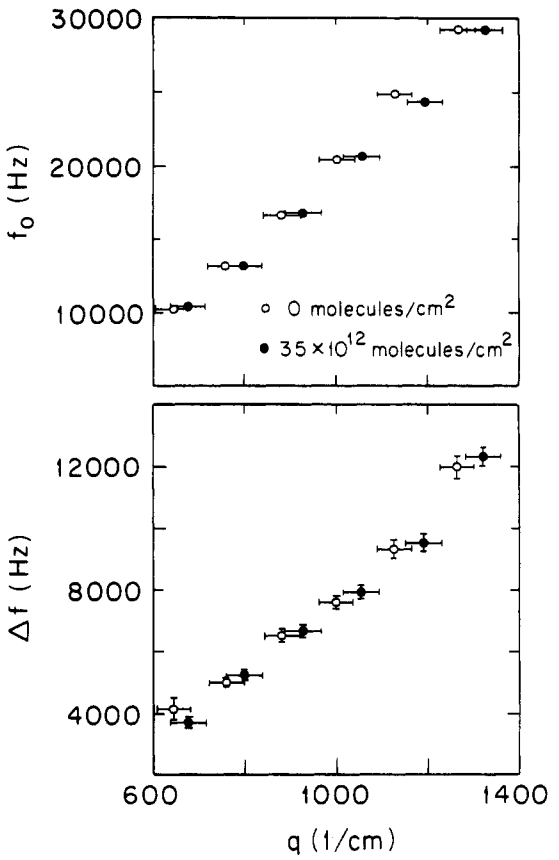

Figure 7. Measured values for power spectra peak frequencies f_o and half-maximum widths Δf versus wavenumber q for two values of the interfacial polymer concentration using 38K M_w PS–PMAA diblock copolymer.

measurements of $\omega^*(q)$ must also obey the dispersion relation, eq 6, and so can be used with eq 6 to determine the surface tension is much the same way as was discussed above for the MGCW case. The SLS values of surface tension presented below have been extracted from D in this way.

IV. Results and Discussion

We present the results of interfacial tension measurements as surface pressures, the magnitudes of the reduction of surface tension due to the presence of the polymer

$$\pi(N) = \sigma(0) - \sigma(N) \quad (13)$$

where N is the polymer surface number density defined above and $\sigma(0)$ is the surface tension of the bare, polymer-free toluene–water interface which we measured to be 36 dyn/cm. Figures 8–10 show the best fit values of π and μ as functions of polymer interfacial number density for polymer molecular weights of 14K, 38K, and 283K, respectively. Each of the three surface pressure curves shows qualitatively the same behavior, with surface pressure increasing from zero as polymer concentration increases until a "saturation" value is reached, beyond which point the surface pressure does not change appreciably. Both the polymer number density at which saturation is reached, N_s, and the saturation surface pressure, π_s, depend on the molecular weight of the polymer. For polymer densities less than N_s, the slope of the surface pressure curve $\partial\pi/\partial N$, increases with molecular weight, indicating a surface layer compressibility ($\kappa' = (1/A)(\partial A/\partial\pi)$ where $A = 1/N$) which, for the lowest number densities, is approximately constant as molecular weight changes. N_s, π_s, and the low concentration values of κ' are listed as a function of molecular weight in Table III. The

Table III. Average Interfacial Properties, As Defined in the Text

M_w	N_s, molecules/cm^2	π_s, dyn/cm	κ', cm/dyn	(N'_s),[a] monomers/cm^2	(ΔE),[b] k_BT/monomer	(A'),[c] Å^2/molecule
14K	4.0×10^{14}	12 ± 1	0.29 ± 0.07	3.2×10^{16}	9.0×10^{-3}	25
38K	1.6×10^{14}	16 ± 1	0.27 ± 0.05	3.2×10^{16}	12×10^{-3}	63
283K	2.0×10^{13}	18 ± 1	0.19 ± 0.03	3.0×10^{16}	15×10^{-3}	500

[a] Saturation monomer density. [b] Energy reduction per monomer. [c] Area per molecule.

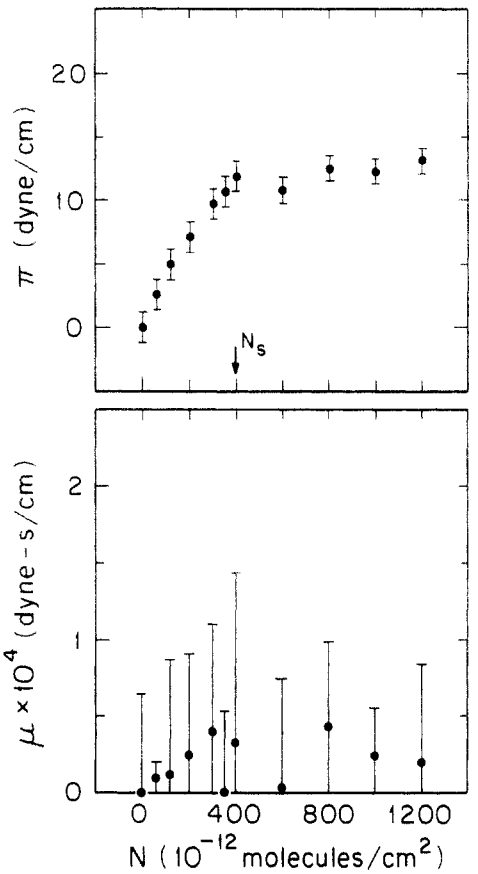

Figure 8. Best-fit surface pressure π and transverse viscosity μ as a function of interfacial polymer density (in molecules/cm^2), obtained using the MGCW technique for the 14K M_w PS–PMAA diblock copolymer.

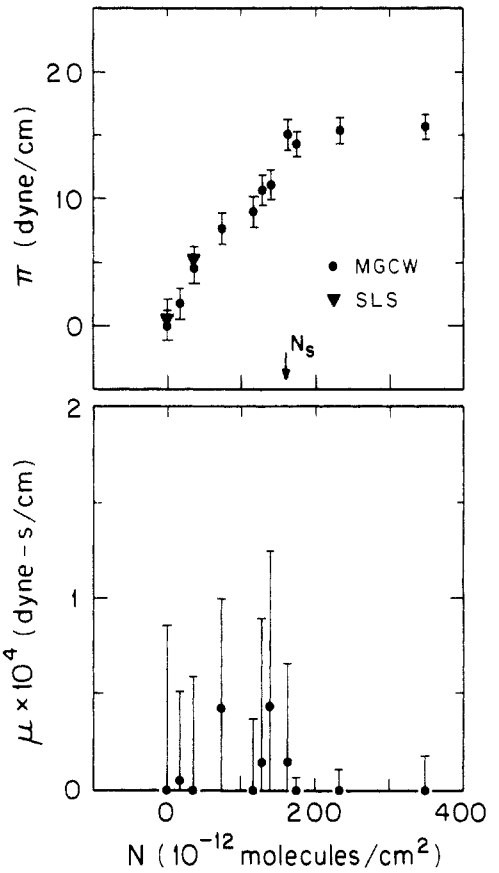

Figure 9. Best-fit surface pressure π and transverse viscosity μ as a function of the interfacial polymer number density (in molecules/cm^2, obtained using both the MGCW and SLS techniques for the 38K M_w PS–PMAA diblock copolymer.

monomer number density at saturation, N'_s is also listed in Table III and can be seen to be approximately the same for all three molecular weights. Column 6 of Table III lists an effective free energy reduction per monomer at saturation for each molecular weight (never more than about 1% of k_BT) and column 7 lists the effective interfacial area per polymer molecule on the assumption that all polymer molecules stay on the interface at concentrations below N_s.

Most of the theoretical work on block copolymers at interfaces has addressed cases where one of the blocks is insoluble and adsorbs at a wall or at an air–liquid interface.[24-30] Bringuier[31] has studied the electrochemical contributions to the free energy and conformation of the polyelectrolyte block of a diblock copolymer on the polar solvent side of a liquid–liquid interface. His results suggest that polyelectrolyte should be stretched, but he does not incorporate in his results neutral layer effects such as have been addressed by Cantor,[32] de Gennes,[33] and Alexander.[34] These effects are similar to those discussed by Halperin and Pincus[35] who predicted that homopolymer will tend to concentrate at the liquid–liquid interface with higher concentration in the better solvent. Pincus[36] considers short polyelectrolyte side chains on a hydrophobic backbone at an oil–water interface, predicting stretched polyelectrolyte chains in the water which form ordered two-dimensional crystal structures at intermediate number densities before forming a melt-like phase at high densities. Other theoretical work has considered the behavior of block copolymers in solutions, including the formation of micelles[37-41] but not including effects from the presence of a liquid–liquid interface. Leibler[42] has incorporated some brief discussion of copolymer behavior at liquid–liquid interfaces in a discussion of interfaces within polymer blends, and Wang and Safran[43] have discussed curvature elasticity for monolayers between incompatible liquids, each of which is a good solvent for one block of the copolymer. Simulations[44-47] have recently become available for liquid–liquid interfaces; these consider solvent exclusion effects alone in reduction of surface tension. While no one available theoretical result incorporates all the features of the present experiment, several possibilities stand out: The copolymers may be strongly attached to the interface since each block is in good solvent; the polyelectrolyte may be fully stretched with significant reduction of free energy from ion formation; there may be some stretching of the nonpolar block at concentrations where the interface is crowded, provided the stretching energy per chain does not become so large as to favor micelle nucleation. (Auroy et al.[48,49] have demonstrated experimentally that chain stretching can be strongly favored for brushes in good solvent, and this could be relevant to the PS blocks in this experiment.) Unfortu-

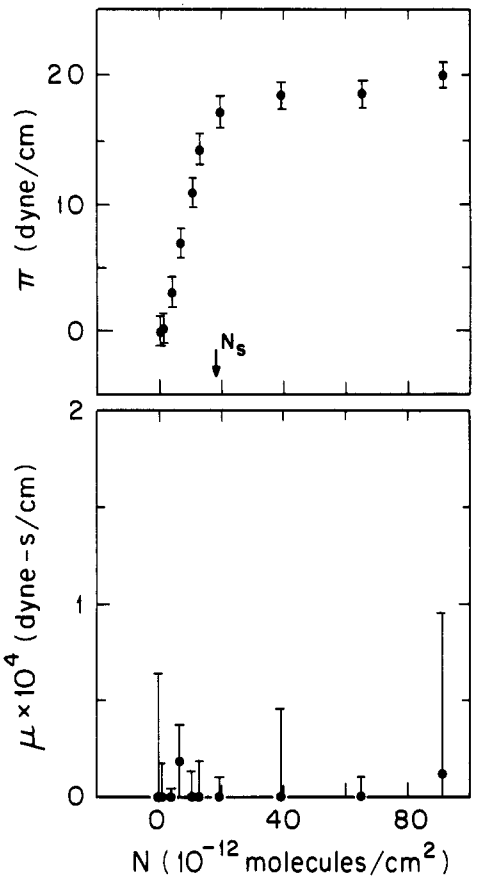

Figure 10. Best-fit surface pressure π and transverse viscosity μ as a function of the interfacial polymer number density (in molecules/cm^2), obtained using the MGCW technique for the 283K M_w PS-PMAA diblock copolymer.

nately, little is known about how high the critical micelle concentration can be pushed by the simultaneous affinity of each polymer block for one of the solvents. Thus the remainder of our discussion of the implications of our measured surface pressure must be tentative.

The easiest speculation to explain the saturation of π is to assume that polymer molecules added after density N_s is reached do not join the interfacial monolayer, i.e., they dissolve into the bulk liquids, possibly forming micelles, or they form multilayered structures at the interface. While this argument is very plausible, and indeed some fraction of the molecules may well be lost to the interfacial monolayer even below N_s, it is interesting and instructive to consider the implications for polymer conformation if a monolayer is formed with true interfacial number density N_s. (This possibility is made more plausible by the observation (in section III above) that scattering centers disappear from the bulk water water and/or the air–water interface when toluene is added in sample preparation at number densities far in excess of N_s. As was discussed in the previous paragraph, the fact that each bulk liquid is a good solvent for one of the polymer blocks may make it very favorable for polymer to crowd onto the liquid–liquid interface.)

The PMAA block is expected to be fully ionized for pH at and above 7. (The data presented herein are all for pH = 7, and no change was observed in the capillary wave spectrum for a test case where KOH was added to bring the water to pH ≈ 9.5.) We estimate the Debye screening length, L_D, to be much larger than the diameter of an MAA monomer (for pH ≈ 7, $L_D \sim 7$ nm) and thus expect the PMAA block to be fully stretched. If all PMAA blocks are fully stretched in an interfacial slab of thickness equal

Table IV. Volume per Chain, Mass Density, and the Polymer Mass Fraction at Saturation for PMAA Blocks if All Molecules Joined an Interfacial Monolayer

M_w	volume per[a] chain, Å^3	mass density, amu/Å^3	polymer mass[b] fraction
14.603K	1.6×10^4	0.49	0.83
38.395K	8.8×10^4	0.20	0.34
283.415K	6.0×10^6	0.03	0.04

[a] This assumes a fully stretched chain with a monomer diameter of 7 Å. [b] This uses the mass density from previous column and divides it by 0.59 amu/Å^3 which is the density of water and is very close to the density of solid polystyrene.

Table V. Radius of Gyration R_G, Approximate Area of Projection of the Blocks, Overlap Number, and the Mass Density for PS Blocks at Saturation if All Molecules Were Unstretched and Joined an Interfacial Monolayer

M_w	R_G, Å	$A = \pi R^2_G$, Å^2	overlap A/A'	mass density,[a] amu/Å^3
14.603K	25	2000	80	11.2
38.395K	46	6600	120	6.6
283.415K	140	62000	125	2.0

[a] This assumes that PS does not stretch but instead sits in a layer of thickness = $2R_G$. As discussed in the text, these densities are unphysically large.

to the length of a stretched chain at saturation, then the volume per chain, the mass density of PMAA, and the polymer mass fraction of the slab would be as listed in Table IV. Table IV shows that the low molecular weight PMAA would be very crowded under these conditions (about ~80% of the density of the bulk material) but that the higher molecular weight PMAA would be much less crowded (about ~4% of bulk density).

Dilute PS in toluene should have a molecular conformation given by a self-avoiding random walk whose radius of gyration, R_G, is given by

$$R_G = 0.137\, M_w^{0.586}\ \text{Å} \qquad (14)$$

where M_w is the molecular weight of the PS block.[50] Table V shows the expected radius of gyration of dilute PS in good solvent for the molecular weights of each of our blocks, the areas of projection on the interface of such well-dissolved blocks, and the number of overlapping molecules at saturation if all the molecules are assumed to be unstretched and participating in an interfacial monolayer. The overlapping of molecules would be large for all cases under these assumptions. The last column in Table V lists the PS mass density at saturation if all PS blocks are assumed to crowd into an interfacial slab of thickness $2R_G$. Even the least dense case exceeds the mass density of bulk PS, an unphysical result which argues very strongly that, as molecules are added to the system near density N_s, some fraction does not join the surface monolayer. However, some of the saturation effect may come from stretching of PS blocks for molecules which do participate in the monolayer, i.e., as an incremental molecule is successfully added to the monolayer near polymer concentration N_s, the reduction in surface free energy from ionizing the relatively uncrowded PMAA block may be comparable to that achieved at much lower density. However, this gain from dissolving PMAA may be offset by energy expended in stretching the PS block, and saturation could result when PS stretching becomes too expensive, beyond which point all additional molecules forced into the system could not join an interfacial monolayer.

In a previous experiment, Sauer et al.[11] measured a decrease in the surface tension of approximately 80% for

their PS–PEO diblock copolymer of M_n 4135 at the heptane/water interface. This was attained at very low surface number density (about 8 molecules would overlap at any one interfacial position if one followed the admittedly dubious procedure of using eq 14 to predict the radius of gyration for such a lower molecular weight). Our maximum decrease in surface tension was observed to be ~50% at M_w = 283K and for the smaller molecular weights the reduction was only ~35%. The discussion of Roe and Rigby[51] anticipates this difference between our case and that of Sauer et al., implying weak surfactant action for polymer blocks too large to be localized at the microscopic liquid interface. Similarly, the calculations of Balazs et al.[44-47] suggest that diblocks of large molecular weight are not well localized at the interface and that the poorest surfactant should be that with the largest molecular weight. The mean-square thickness of an interface between two liquids should be[52]

$$\langle \xi \rangle^2 = \frac{k_B T}{\sigma} \tag{15}$$

where σ is the bare liquid surface tension. For toluene and water at room temperature this implies a half thickness of 0.22 nm while the radius of gyration of the smallest block used in this experiment is 11 times larger (2.5 nm).

On the other hand, within our group of large molecules, the trend is different, with the largest surface tension reduction coming from the largest molecular weight and the smallest number of "tethered" points (tethered in the sense that the point of juncture of the two blocks is presumably constrained to stay rather close to the liquid interface). Roe and Rigby[51] and Balazs et al.[44-47] considered only solvent exclusion in reducing surface tension, and that may not be the most important feature in calculating changes in the free energy of an interface decorated with long chain diblocks; instead, as was discussed above, ionization of monomers, distribution of counterions, and chain conformation energy in good solvent may all contribute strongly to the net reduction of the free energy density in the immediate vicinity of the interface.[31-43]

For the MGCW data, the transverse viscosity μ is consistent with zero (to great accuracy, of order 10^{-5} dyn·s/cm, since the measurement is directly observing the transverse waves). As was mentioned above, the SLS data are only consistent with $\mu = 0$ (to similar accuracy) if the instrumental line width is assumed to be significantly larger than that which would correspond to the measured width of the reference beam at a given diffraction order. Since this arbitrary increase in experimental line width is necessary to achieve the physically reasonable result that $\mu = 0$ when there is no polymer on the interface, we conclude that the SLS results do not contradict the MGCW results and that $\mu = 0\ (+1, -0 \times 10^{-5})$ dyn·s/cm for all molecular weights and number densities measured in this study. In their previous study of very low molecular weight PS–PEO diblock copolymer at the heptane/water interface, Sauer et al.[11] report $\mu = (0 \pm 5) \times 10^{-6}$ dyn·s/cm.

Because some other investigations have reported frequency-dependent viscoelastic parameters,[19] we obtained values for the surface tension σ and transverse viscosity μ which best fitted each SLS power spectrum at definite wavenumber q and best fitted each MGCW capillary wave profile at definite frequency f. The average values obtained from this analysis agree well with and have similar uncertainties to those obtained through the global fits discussed above. We do not observe any frequency dependence in the surface tension σ in the wavenumber/

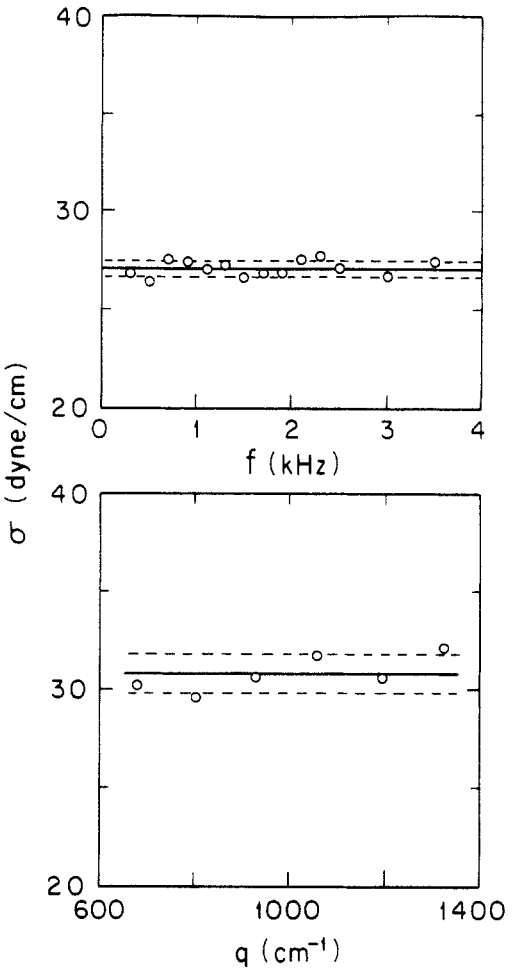

Figure 11. Surface tension σ versus (a) frequency obtained using the MGCW technique at 116×10^{12} molecules/cm^2 of 38K M_w PS–PMAA diblock copolymer and (b) wavenumber using the SLS technique for 35×10^{12} molecules/cm^2 of 38K M_w PS–PMAA diblock copolymer. The solid line shows the best-fit value for σ and the dashed lines are at 1 standard deviation.

frequency range analyzed here, as shown both for MGCW data and SLS data in Figure 11. Neither do we observe any significant frequency dependence of the transverse viscosity μ for MGCW measurements.

As was mentioned above, the densities and viscosities of toluene and water are too similar to allow us significant sensitivity to the moduli ϵ and κ which describe the longitudinal waves on the interface. As a result, the uncertainties in our best fits to these parameters are large, with the global fits constraining them only crudely. κ, the viscosity associated with longitudinal waves, is always consistent with 0; the uncertainty in κ is typically ~10^{-4} dyn·s/cm. ϵ always has very large uncertainty (a few dyn/cm) and is at most polymer densities consistent with $\epsilon = 0$. Even though ϵ is at some densities slightly more than 1 standard deviation above zero, it is best regarded as consistent with zero and bounded above by ~12 dyn/cm. If one assigns an area per molecule as the inverse polymer number density and calculates the expected value of ϵ as $\epsilon = A(\partial\sigma/\partial A)$,[53] the expected values vary from 0 to 5 dyn/cm and so are never inconsistent with the limits established by our experiment.

The region of greatest sensitivity to the parameters κ and ϵ occurs at frequencies around 200–300 Hz for the toluene/water interface.[18] This is where the wavenumbers of the capillary waves and the longitudinal waves are approximately equal and where the relative maxima in the measured wavenumber and damping constant are

largest. This sensitivity at low frequencies probably explains why our MGCW data yield as much information as we have been able to extract with only marginal extra confidence arising from extending the frequency/wavenumber range into the region supplied by the SLS measurements.

We have also performed an experiment in which we compared the wavenumber q and damping constant β obtained from MGCW measurements when the wire was driven horizontally (in the plane of the interface) and when it was driven vertically (perpendicular to the interface). Horizontal driving might be expected to place an increased amount of energy in the longitudinal waves with possible differences in the behavior of the transverse waves if any significant nonlinearity is involved in the coupling, i.e., the onset of differences between the two driving motions might be used as a test for the onset of nonlinear dynamical effects in the wave motion. However, we measured no significant differences in q and β at any frequency for the two cases.

V. Summary

We have measured the capillary wave dispersion relation for a toluene/water interface covered with PS-PMAA diblock copolymer over a wide frequency range using both a mechanically generated capillary wave technique and surface light scattering. Using these measurements and the expected functional form of the dispersion relation for a thin viscoelastic interfacial layer between two layers of simple liquids, we have determined the surface tension and surface transverse viscosity of the interfacial layer as a function of polymer number density and molecular weight. Surface tension has been presented as surface pressure (surface tension reduction) π. Crude limits have also been placed on ϵ and κ, the moduli for longitudinal waves.

Interesting changes in the surface pressure π have been observed: as the interfacial polymer number density N is increased, π increases with a slope dependent upon molecular weight and reaches a maximum value at a particular interfacial density (saturation density), beyond which density π no longer changes appreciably. The slope of $\pi(N)$ indicates that large and small molecules show approximately the same areal compressibility at the lowest number densities. The saturation surface pressure is larger for the highest molecular weight than for the two lower M_w polymers despite the fact that such large molecules should be less effective in excluding the incompatible solvents from contacting each other. Saturation densities decrease as molecular weight increases, in such a way as to give saturation at approximately the same overall monomer density for each molecular weight.

Acknowledgment. We acknowledge helpful discussions with A. C. Balazs, J. S. Huang, D. Jasnow, P. A. Pincus, and T. A. Witten. This work was supported by the National Science Foundation through Grant No. DMR-9001518.

References and Notes

(1) Gaines, G. L., Jr. *Langmuir* **1991**, *7*, 834.
(2) Conner, M.; Kudelka, I.; Regen, S. L. *Langmuir* **1991**, *7*, 982.
(3) Schlossman, M. L.; Schwartz, D. K.; Kawamoto, E. H.; Kellogg, G. J.; Pershan, P. S.; Kim, M. W.; Chung, T. C. *J. Phys. Chem.* **1991**, *95*, 6628.
(4) Gentle, I. R.; Saville, P. M.; White, J. W.; Penfold, J. *Langmuir* **1993**, *9*, 646.
(5) Bringuier, E.; Vilanove, R.; Gallot, Y.; Selb, J.; Rondelez, F. *J. Colloid Interface Sci.* **1985**, *95*, 104.
(6) Sauer, B. B.; Yu, H.; Kim, M. W. *Langmuir* **1989**, *5*, 278.
(7) Zhu, J.; Eisenberg, A.; Lennox, R. B. *J. Am. Chem. Soc.* **1991**, *113*, 5583.
(8) Zhu, J.; Lennox, R. B.; Eisenberg, A. *Langmuir* **1991**, *7*, 1579.
(9) Li, S.; Hanley, S.; Khan, I.; Varshney, S. K.; Eisenberg, A.; Lennox, R. B. *Langmuir* **1993**, *9*, 2243.
(10) Shull, K. R. *Macromolecules* **1993**, *26*, 2346.
(11) Sauer, B. B.; Yu, H.; Tien, C.; Hager, D. F. *Macromolecules* **1987**, *20*, 393.
(12) Cosgrove, T.; Phipps, J.; Richardson, R. M. *Colloids Surf.* **1992**, *62*, 199.
(13) Måløy, K. J.; Feder, J.; Jøssang, T. *Rev. Sci. Instrum.* **1989**, *60*, 481.
(14) Polymer Laboratories, Inc., Amherst MA 01002.
(15) Klesper, E.; Gronski, W.; Barth, V. *Makrolmol. Chem.* **1971**, *139*, 1.
(16) Leiderer, P.; Poisel, H.; Wanner, M. *J. Low Temp. Phys.* **1977**, *28*, 167.
(17) G. Finkenbeiner Co., Waltham, MA 01002.
(18) May, S. E. Ph.D. Thesis, University of Pittsburgh, 1992 (unpublished).
(19) Langevin, D. In *Light Scattering by Liquid Surfaces Complementary Techniques*; Langevin, D., Ed.; Marcel Dekker, Inc.: New York, 1992.
(20) Lucassen-Reynders, E. H.; Lucassen, J. *Adv. Colloid Interface Sci.* **1969**, *2*, 347.
(21) Harden, J. L.; Pleiner, H.; Pincus, P. A. *J. Chem. Phys.* **1991**, *94*, 5208.
(22) Press, W. H.; Flannery, B. P.; Teukolsky, S. A.; Vetterling, W. T. *Numerical Recipes-The Art of Scientific Computing*; Cambridge University Press: New York, 1985.
(23) Hård, S.; Hamnerius, Y.; Nilsson, O. *J. Appl. Phys.* **1976**, *47*, 2433.
(24) Munch, M. R.; Gast, A. P. *Macromolecules* **1988**, *21*, 1366.
(25) Marques, C.; Joanny, J. F.; Leibler, L. *Macromolecules* **1988**, *21*, 1051.
(26) Muthukumar, M.; Ho, J. S. *Macromolecules* **1988**, *21*, 1051.
(27) Milner, S. T.; Wang, Z. G.; Witten, T. A. *Macromolecules* **1989**, *22*, 1454.
(28) Marques, C. M.; Joanny, J. F. *Macromolecules* **1989**, *22*, 1454.
(29) Rossi, G.; Cates, M. E. *Macromolecules* **1988**, *21*, 1372.
(30) Milner, S. T.; Witten, T. A.; Cates, M. E. *Macromolecules* **1988**, *21*, 2610.
(31) Bringuier, E. *J. Phys. Lett.* **1984**, *45*, L107.
(32) Cantor, R. *Macromolecules* **1981**, *14*, 1186.
(33) de Gennes, P. G. Molecular Films on Block copolymers; Theoretical Equation of State (1975) (unpublished).
(34) Alexander, S. J. *J. Phys. (Paris)* **1977**, *38*, 938.
(35) Halperin, A.; Pincus, P. A. *Macromolecules* **1986**, *19*, 79.
(36) Pincus, P. *J. Colloid Interface Sci.* **1978**, *63*, 561.
(37) Frederickson, G. H.; Leibler, L. *Macromolecules* **1989**, *22*, 1238.
(38) Munch, M. R.; Gast, A. P. *Macromolecules* **1988**, *21*, 1360.
(39) Leibler, L.; Orland, H.; Wheeler, J. C. *J. Chem. Phys.* **1983**, *79*, 3550.
(40) Dan, N.; Tirrell, M. *Macromolecules* **1993**, *26*, 637.
(41) Marko, J. F.; Rabin, Y. *Macromolecules* **1992**, *25*, 1503.
(42) Leibler, L. *Phys. A* **1991**, *172*, 258.
(43) Wang, Z. G.; Safran, S. A. *J. Chem. Phys.* **1991**, *94*, 679.
(44) Balazs, A. C.; Siemasko, C. P.; Lantman, C. W. *J. Chem. Phys.* **1991**, *94*, 1653.
(45) Balazs, A. C.; Zhou, Z. X.; Yeung, C. *Langmuir* **1992**, *8*, 2295.
(46) Li, W. X.; Yeung, C.; Jasnow, D.; Balazs, A. C. *Macromolecules* **1992**, *25*, 3685.
(47) Yeung, C.; Balazs, A. C.; Jasnow, D. *Macromolecules* **1992**, *25*, 1357.
(48) Auroy, P.; Auvrey, L.; Léger, I. *Phys. Rev. Lett.* **1991**, *66*, 719.
(49) Auroy, P.; Auvrey, L.; Léger, L. *Phys. A* **1991**, *172*, 269.
(50) Berry, G. C. *J. Chem. Phys.* **1966**, *4*, 4550.
(51) Roe, R. J.; Rigby, D. In *Advances in Polymer Science*; Springer-Verlag: New York, 1989; Vol. 82.
(52) Moldover, M. R. *Phys. Rev. A* **1985**, *31*, 1022.
(53) Vogel, V.; Möbious, D. *Langmuir* **1989**, *5*, 129.
(54) Harden, J. L.; Pleiner, H.; Pincus, P. A. *Langmuir* **1989**, *5*, 1436.